

Investigating the Longitudinal Optical Conductivity in Three-Layer Graphene Systems with Composites Mono-Bi-Bi and Bi-Mono-Bi and Bi-Bi-Mono

M. H. Feizi Derakhshi^{1,}, H. Ghaffari²*

^{1,2}Department of Physics, Tabriz Branch, Islamic Azad University, Tabriz, Iran

Received: 9 March 2020; Accepted: 12 May 2020

ABSTRACT: The longitudinal optical conductivity is the most important property for graphene-based devices. So investigating this property for spatially separated few-layer graphene systems analytically and numerically is the main purpose of our study. Each layer can be mono- or bi-layer graphene. The density-density correlation function has been screened by the dielectric function using the random phase approximation, which includes the inter-layer Coulomb coupling. By using Kronecker delta and dielectric tensors, the optical conductivity, is calculated, and plotted as a function of photon energy for three-layer graphene systems with composites mono-bi-bi, bi-mono-bi, and bi-bi-mono in different broadening widths. In the presence of the potential function between the layers, the carrier densities in each layer can be tuned respectively. In these two dimensional layered structures; the main contributions to the optical conductivity are from the intra- and inter-band transition channels in a same layer.

Keywords: *Electron density, Fermi Energy, Optical conductivity, Three-layer Graphene.*

INTRODUCTION

Graphene, single atomic layer thickness, was fabricated experimentally by Geim, et al. This ultra-thin material exhibits very exceptional and excellent physical properties, such as, Klein tunneling, high mobilities, unique quantum Hall effect, and so on. Using the applied field (or gate voltage) the carrier density can be tuned, and the corresponding transport properties can be measured experimentally. For example, using the global gate and a metallic top gate in single layer graphene, which led to the electrostatic potential barrier, n-p junctions with tunable charge densities can be obtained and the transport measurements in the presence of barrier can be

performed experimentally. In the presence of the barrier structure, the charge transmission coefficient depends on the height and the width of the barrier and transmittance value is less than one. But for graphene material, owing the suppression of backscattering, the charge exhibits perfect transmission through the barrier at normal incidence regardless of the barrier characteristics. During the fabrication of graphene material, the number of graphene layer has many possibilities, such as, mono-layer, bi-layer, and few-layers. For example, mono-bi-bi, means the first layer is formed by one sheet of graphene, while the second and third layers are made of two sheets of graphene. In a more than one-

(*) Corresponding Author - e-mail: h_ghafari@iaut.ac.ir

layer system with top and back gates, the out-of-plane electric field creates a different potential between the layers and the carriers densities in each layer can be independently controlled by gates. The carrier density in each layer can be obtained by the capacitance between graphene and the gates. Some ultra-thin dielectric layers can be used to separate graphene layers into two or more independently contacted single- or bi-layers. The dependence of the layer resistivities on the back gate bias indicates that the charge densities in each graphene layers are induced differently with the applied back gate voltage. At the Fermi energy, the kinetic energy in a different layer is different. Khrapach et al., intercalated the FeCl_3 into two- to five-layer graphene [1-3]. The Raman spectra measurements indicate the decoupling of the few layer graphene. The longitudinal magneto-conductance oscillates as a function of perpendicular magnetic field at $T < 10\text{K}$, which indicates the distinct charge densities in different layers. From the Hall resistance measurement, it has found that the monolayer and bilayer graphene are included in the intercalation graphene system. The optical transmission in the visible wavelength range slightly decreases at low wavelength. Bao et.al. demonstrated an increase of optical transmittance in the visible range upon Lithium intercalation for 3-60 graphene layers, which is explained by the suppression of interband transitions. Min et.al. calculated the static polarizability and screening of multilayer graphene which is dependent on the layer number and includes the intra- and inter-band polarizability. The theoretical Thomas-Fermi screening wave vector results show different behaviours for several stacking sequences which implies the importance of the layer structure. Das Sarma et al., investigated the intrinsic and extrinsic plasmons for single- and double-layer systems and the effects of the layered structure, electron densities, the background lattice dielectric constant, and the temperature are included in their investigations. The optical conductivity in graphene also exhibits other important properties with inter- and intra-band transitions channels which have been widely investigated experimentally and theoretically. The experimental value of the optical conductivity per graphene layer (or an optical sheet conductivity) is almost a constant and close to $\sigma_0 = e^2/4h$, above $2E_f$, which is indepen-

dent from the frequency and the inter-layer hopping. The second observation is that the optical sheet conductivity showed a threshold structure at two times the Fermi energy under an applied gate voltage and the turning points can be tuned by the gate voltage. Theoretically, the Boltzmann transport theory and/or the Kubo formula were employed to investigate the optical conductivity as a function of the gate voltage and the optical frequency with the disorder broadening from impurity and phonon scattering. The optical conductivity is proportional to the layer number multiplying the universal optical conductivity. Taking into account of the full energy dispersion, the results for the optical conductivity from the infrared to the ultra-violet frequency regions are obtained with extra peak structures observed [1].

In this paper, the structures with three isolated parallel two dimension mono-layer graphene, in combination with two bi-layer graphene, separated by a distance d with an ultra-thin dielectric is studied. When an inter-layer distance d is about a few angstroms ($d \sim 3.5 \text{ \AA}$), the out-of-plane π orbitals from two adjacent graphene sheets start to overlap. The inter-layer tunneling is obvious when ($d \sim 1-5 \text{ \AA}$). Increasing the distance between the adjacent layers, the inter-layer tunneling decreases, and inter-layer electron-electron Coulomb scattering should be included. Here, we refer to the electron systems (i.e. extrinsic graphene systems) where the Fermi energy $E_f > 0$ and $T \rightarrow 0$. The carrier density for each layer can be tuned both by the chemical doping and applied field (or gate voltage). The carrier densities each layer can be independently controlled by using top and bottom gates. The carrier density in each layer can be obtained by the capacitance between graphene and the gates.

THEORETICAL APPROACHES

For a several-layer graphene system, using the mean-field random phase approximation, The dielectric tensor ϵ_n , and its elements, $\epsilon_{l,m}(q,\omega)$, where $l,m=1,2,\dots,n$ denoting the different layer, can be written as:

$$\epsilon_n = \Delta_n - V_n \Pi_n$$

$$\epsilon_n = \begin{bmatrix} \epsilon_{11} & \epsilon_{12} & \epsilon_{13} & \dots & \epsilon_{1n} \\ \epsilon_{21} & \epsilon_{22} & \epsilon_{23} & \dots & \epsilon_{2n} \\ \epsilon_{31} & \epsilon_{32} & \epsilon_{33} & \dots & \epsilon_{3n} \\ \vdots & \vdots & \vdots & \dots & \vdots \\ \epsilon_{n1} & \epsilon_{n2} & \epsilon_{n3} & \dots & \epsilon_{nn} \end{bmatrix}$$

$$\Delta_n = \begin{bmatrix} \delta_{11} & \delta_{12} & \delta_{13} & \dots & \delta_{1n} \\ \delta_{21} & \delta_{22} & \delta_{23} & \dots & \delta_{2n} \\ \delta_{31} & \delta_{32} & \delta_{33} & \dots & \delta_{3n} \\ \vdots & \vdots & \vdots & \dots & \vdots \\ \delta_{n1} & \delta_{n2} & \delta_{n3} & \dots & \delta_{nn} \end{bmatrix}$$

Where the elements $\delta_{l,m} = \begin{cases} 1, l=m \\ 0, l \neq m \end{cases}$ are Kronecker deltas, Showing the Identity matrix. V_n the Coulomb interaction tensor;

$$V_n = \begin{bmatrix} v_{11} & v_{12} & v_{13} & \dots & v_{1n} \\ v_{21} & v_{22} & v_{23} & \dots & v_{2n} \\ v_{31} & v_{32} & v_{33} & \dots & v_{3n} \\ \vdots & \vdots & \vdots & \dots & \vdots \\ v_{n1} & v_{n2} & v_{n3} & \dots & v_{nn} \end{bmatrix} = \alpha \begin{bmatrix} \beta^0 & \beta^1 & \beta^2 & \dots & \beta^{n-1} \\ \beta^1 & \beta^0 & \beta^1 & \dots & \beta^{n-2} \\ \beta^2 & \beta^1 & \beta^0 & \dots & \beta^{n-3} \\ \vdots & \vdots & \vdots & \dots & \vdots \\ \beta^{n-1} & \beta^{n-2} & \beta^{n-3} & \dots & \beta^0 \end{bmatrix}$$

Here, $\alpha = V_q = 2\pi e^2/kq$ is the intra_layer Coulomb interaction, κ is the static dielectric constant for $\beta = e^{-qd}$, In which, d is the distance between the adjacent layers. So we can write $V_n = \alpha \beta^n$, Π_n is the density_density correlation tensor. For a several_layer graphene system, each layer separated by a dielectric $\pi_{lm} = 0$, if $l \neq m$, and $\pi_{lm} = \pi_l$, if $l = m$. We can obtain:

$$\Pi_n = \begin{bmatrix} \pi_1 & 0 & 0 & \dots & 0 \\ 0 & \pi_2 & 0 & \dots & 0 \\ 0 & 0 & \pi_3 & \dots & 0 \\ \vdots & \vdots & \vdots & \dots & \vdots \\ 0 & 0 & 0 & \dots & \pi_n \end{bmatrix}$$

The matrix elements $\pi_l = \pi_l(q, \omega)$ are the density-density correlation functions, which for mono- and bilayer graphene can be obtained as:

$$\pi_l(q, \omega) = g_s g_v \sum_{s,s',k_m} \frac{1 + ss' A_{k_m q}}{2} \frac{f_{s,k_m} - f_{s',k_m+q}}{\hbar\omega + E_{s,k_m} - E_{s',k_m+q} + i\Gamma_m}$$

$g_s = 2$ is spin degeneracy. There are two points k and k' at the corner of the graphene Brillouin zone, called the Dirac points. $g_v = 2$ refers to this degeneracy, f_{s,k_m} is the Fermi-Dirac distribution function in the m -th layer. $s, s' = \pm 1$ refer to the conduction band (+1) and the valence band (-1). $1 + ss' A_{k_m q} / 2$ comes from the overlap of

carrier states. $A_{k_m q} = \cos\varphi_m$ and $A_{k_m q} = \cos 2\varphi_m$ in mono-layer and bilayer graphene respectively, $\cos\varphi_m = k_m + q \cos\theta_m / |k_m + q|$, θ_m being the angle between k_m and q . In monolayer graphene, $E_{s,k} = \hbar v_F |k|$ (v_F being the Fermi velocity of graphene). In bilayer graphene $E_{s,k} = \hbar^2 k^2 / 2m$, $m \approx 0.033$ is the effective mass of bilayer graphene with m_e being the free-electron mass. Γ_m is the broadening width induced by the carrier scattering process. For a three-layer graphene system we obtain that:

Graphene, $\beta_{lm} = \beta^{|l-m|}$, and $\epsilon_3 = \Delta_3 - V_3 \Pi_3$

$$\Pi_3 = \begin{bmatrix} \pi_1 & 0 & 0 \\ 0 & \pi_2 & 0 \\ 0 & 0 & \pi_3 \end{bmatrix}$$

So we can write:

$$\epsilon_3 = -V_q \begin{bmatrix} 1 - \frac{1}{V_q \pi_1} e^{-qd} & e^{-2qd} \\ e^{-qd} & 1 - \frac{1}{V_q \pi_2} e^{-qd} \\ e^{-2qd} & e^{-qd} & 1 - \frac{1}{V_q \pi_3} \end{bmatrix} \begin{bmatrix} \pi_1 & 0 & 0 \\ 0 & \pi_2 & 0 \\ 0 & 0 & \pi_3 \end{bmatrix}$$

Then ϵ_3 becomes as;

$$\epsilon_3 = \begin{bmatrix} 1 - V_q \pi_1 & -V_q e^{-qd} \pi_2 & -V_q e^{-2qd} \pi_3 \\ -V_q e^{-qd} \pi_1 & 1 - V_q \pi_2 & -V_q e^{-qd} \pi_3 \\ -V_q e^{-2qd} \pi_1 & -V_q e^{-qd} \pi_2 & 1 - V_q \pi_3 \end{bmatrix}$$

Determination of the dielectric matrix function for three-layer graphene system yields;

$$\epsilon_3(q, \omega) = 1 - V_q [\pi_1 + \pi_2 + \pi_3] + V_q^2 (1 - e^{-2qd}) [\pi_1 \pi_2 + \pi_2 \pi_3] + V_q^2 (1 - e^{-4qd}) [\pi_1 \pi_3] + V_q^3 (1 - 2e^{-2qd} + e^{-4qd}) [\pi_1 \pi_2 \pi_3]$$

Knowing that; $\pi_l = \pi_l(q, \omega)$. And we find imaginary part of dielectric function as;

$$\text{Im} \epsilon_3(q, \omega) = -V_q [\text{Im} \pi_1 + \text{Im} \pi_2 + \text{Im} \pi_3] + V_q^2 (1 - e^{-2qd}) [\text{Im} \pi_1 \pi_2 + \text{Im} \pi_2 \pi_3] + V_q^2 (1 - e^{-4qd}) [\text{Im} \pi_1 \pi_3] + V_q^3 (1 - 2e^{-2qd} + e^{-4qd}) [\text{Im} \pi_1 \pi_2 \pi_3]$$

The longitudinal optical conductivity can be obtained by the dielectric function [2].

$$\sigma_{xx}(\omega) = -e^2 \omega \lim_{q \rightarrow 0} \frac{1}{q^2} \sum_m \text{Im} \frac{\pi_m(q, \omega)}{\epsilon(q, \omega)}$$

$\epsilon(q, \omega)$ is the determination of the dielectric-matrix

function. ω is the frequency of the incident-light. $q \rightarrow 0$ reflects a fact that the electron-photon scattering does not change the wave vector of an electron, which can be understood from Maxwell equations with a complex dielectric function $\varepsilon' = \varepsilon + i\sigma/\omega$ being introduced to investigate the optical absorption problems. The longitudinal optical conductivity $\sigma_{xx}(\omega)$ is proportional to $(\text{Im}\pi\text{Re}\varepsilon - \text{Im}\varepsilon\text{Re}\pi)$. The intra- and inter-band d-d correlation functions contribute to the real and imaginary parts.

$$\pi_{L,i}(q, \omega) = R_e \pi_{L,i}(q, \omega) + I_m \pi_{L,i}(q, \omega)$$

Each part can be written as

$$R_e \pi_{L,i}(q, \omega) = R_e \pi_{L,i}^{++}(q, \omega) + R_e \pi_{L,i}^{--}(q, \omega)$$

$$I_m \pi_{L,i}(q, \omega) = I_m \pi_{L,i}^{++}(q, \omega) + I_m \pi_{L,i}^{--}(q, \omega)$$

The real parts in the i -th layer are

$$R_e \pi_{L,i}^{++}(q, \omega) = L \frac{g_s g_v E_f^i q^2}{4\pi(\hbar\omega)^2} \frac{1 - x_i^2}{(1 + x_i^2)}$$

and

$$R_e \pi_{L,i}^{--}(q, \omega) = L \frac{g_s g_v q^2}{16\pi} \left[\frac{\hbar\omega}{2A_i} \ln \frac{k^{2L}}{R_i} + \left(\frac{(\hbar\omega)^2}{A_i} - 1 \right) \frac{1}{\Gamma_i} \tan^{-1} \frac{\Delta}{\Gamma_i} \right]_{k_i^j}^{k_c}$$

The imaginary parts are

$$I_m \pi_{L,i}^{++}(q, \omega) = -L \frac{g_s g_v E_f^i q^2 \Gamma_i}{2\pi(\hbar\omega)^3}$$

$$I_m \pi_{L,i}^{--}(q, \omega) = -L \frac{g_s g_v q^2 \Gamma_i}{16\pi A_i} \left[\frac{1}{2} \ln \frac{k^{2L}}{R_i} + \frac{\hbar\omega}{\Gamma_i} \tan^{-1} \frac{\Delta}{\Gamma_i} \right]_{k_i^j}^{k_c}$$

(++) and (--) denoting intra- and inter channel transitions, respectively. Here $L=1, 2$ is for monolayer and bilayer graphene respectively. This coefficient is similar to the obtained plasmon results in MLG and BLG. These two plasmon analytical results are identical except for an extra factor of $\sqrt{2}$ in the BLG case. $x_i = \Gamma_i/\hbar\omega$, $A_i = (\hbar\omega)^2 + \Gamma_i^2$, $\Delta = 2\gamma k - \hbar\omega$, $R_i = (2\gamma k - \hbar\omega)^2 + \Gamma_i^2$, $\gamma = \hbar v_f$ and k_c is the cutoff wave vector above which the linear energy dispersion approximation breaks down for graphene. $k_c \sim 1/a$ (a being the distance between C-C bond). The real and imaginary parts of intra- or inter-band d-d correlation function have much common factors, and have similar relationship to the broadening width, Fermi energy, q -wave vector, and the optical frequency. Using the imaginary parts of the d-d correlation function and the dielectric function, results of the optical conductivity $\sigma_{xx}(\omega)$ can be ob-

tained by the analytical calculation. The contributions to the optical conductivity are from electron-hole excitations from the intra-layer and inter-layers. In each

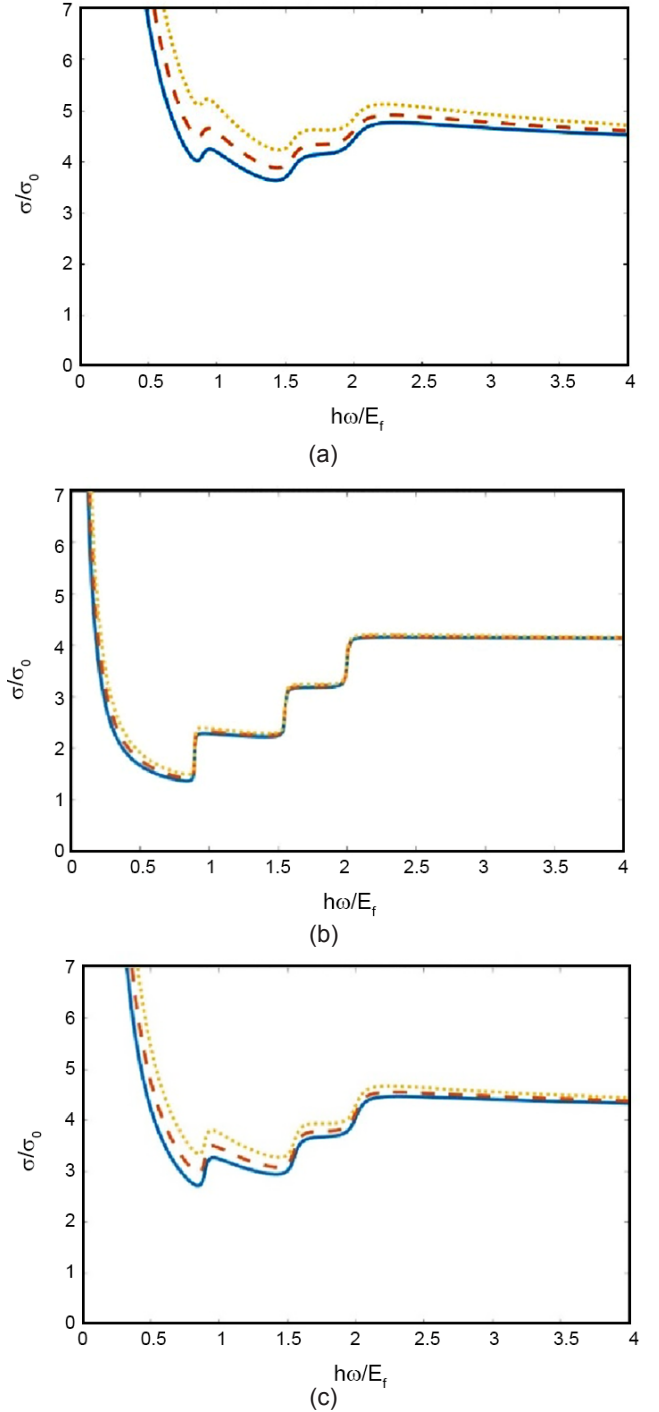


Fig. 1. The optical conductivity as a function of photon energy, for Three-layer graphene systems mono-bi-bi (solid line), and bi-mono-bi (dash line), and bi-bi-mono (dot line) in different broadening widths width values; a) $\Gamma = 0.09 E_f$; b) $\Gamma = 0.05 E_f$; c) $\Gamma = 0.01 E_f$; $n_1 = 5 \times 10^{12} \text{ cm}^{-2}$; $n_2 = 3 \times 10^{12} \text{ cm}^{-2}$, $n_3 = 1 \times 10^{12} \text{ cm}^{-2}$ are electron densities in first-, second-, and third-layers respectively.

layer, there are two transition channels (intra- and inter-band transitions) contributing to the optical absorption. When the applied optical field drive is present, the carriers are excited from the occupied states to the unoccupied states. The intra-band contribution corresponds to electron excitation in the vicinity of the Fermi level within the conduction band. While the inter-band contribution corresponds to carrier excitation from the valance band to the conduction band and has a turning point at $2E_F$. These two processes are intra-layer case given by the V_q term. The inter-layer contributions given by V_q^2 , V_q^3 terms. The carriers are driven by the electric field force, through the Coulomb scattering, and the momentum is transferred to the adjacent layers which drive the carriers. But this strength decreases with increasing the distance between the two layers. The optical conductivity becomes:

$$\sigma_{xx}(\omega) = \omega l_m \epsilon_3(q, \omega)$$

Gate voltage can be used to tune the carrier density and the electrons are occupied. In limits of long wavelength (i.e., $q \rightarrow 0$), the inter-layer contribution is smaller than the intra-layer contribution by e^{-qd} factor. And the intra-band contribution is smaller than the inter-band contribution when the optical energy is larger than two times the kinetic energy at the Fermi energy. This is because, in the presence of the optical field, the electrons absorbing the optical energy are excited to the above unoccupied states, satisfying the conditions of the conservation of momentum. Inter-band channels have higher probabilities to achieve these processes.

RESULTS AND DISCUSSION

Theoretical investigations using dielectric tensor which has been obtained from electron density-density correlation function, leading to numerical analysis and methods. We used a MATLAB program to calculate

the total optical conductivity, and plotted it as a function of photon energy for different broadening widths and constant electron densities in each layer. The total optical conductivity can be calculated from imaginary part of three-layer graphene dielectric function. The results have been collected and shown as below;

APPROACHES AND FINDINGS

By comparing Figs. 1, 2 and 3 can be observed;

- 1- The values of longitudinal optical conductivity, for different composes of three-layer graphene systems are; $\sigma_{mmb} > \sigma_{bmb} > \sigma_{bbm}$
- 2- Coming up the one sheet thick graphene layer, the slide of first threshold structure is less in value.
- 3- At high energy regions, the optical conductivity of all three-layer systems tendency to five times of a sheet graphene's optical conductivity.
- 4- By decreasing the value of broadening width, turning regions between different threshold structures, sharply increase.
- 5- By decreasing the value of broadening width, the value of the optical conductivity decreases too.
- 6- Decreasing the value of broadening width, causes decreasing of curve slide in all compose.

REFERENCES

- [1] Yang, C.H., Chen, Y.Y., Jiang, J.J., Ao, Z.M. (2016). The optical conductivity in double and three layer graphene systems. *Solid State Commun.*, 227, 23-27.
- [2] Hwang, E.H., Das Sarma, S. (2009). Plasmon modes of spatially separated double-layer graphene. *Phys. Rev. B*, 80, 205406.
- [3] Yang, C.H., Wan, P., Li, Q.F., Ao, Z.M. (2016). Coulomb screening effects on the optoelectronic far-infrared properties of spatially separated few-layer graphene. *Physica E*, 84, 324-329.

AUTHOR (S) BIOSKETCHES

M.H. Feizi Derakhshi, Department of Physics, Tabriz Branch, Islamic Azad University, Tabriz, Iran,
Email: h_ghafari@iaut.ac.ir

Hossein Ghaffari, Department of Physics, Tabriz Branch, Islamic Azad University, Tabriz, Iran, *Email:*
h_ghafari@iaut.ac.ir